

# Dynamic Performance Analysis of Hysteresis Motors by a Linear Time-Varying Model

A. Darabi\*, T. Ghanbari\*, M. Rafiei\*, H. Lesani\*\* and M. Sanati-Moghadam\*

**Abstract:** Hysteresis motors are self starting brushless synchronous motors which are being used widely due to their interesting features. Accurate modeling of the motors is crucial to successful investigating the dynamic performance of them. The hysteresis loops of the material used in the rotor and their influences on the parameters of the equivalent circuit are necessary to be taken into consideration adequately. It is demonstrated that some of the equivalent circuit parameters vary significantly with input voltage variation and other operating conditions. In this paper, a comprehensive analysis of a hysteresis motor in the start up and steady state regimes are carried out based on a developed d-q model of the motor with time-varying parameters being updated during the simulation time. The equivalent circuit of the motor is presented taking into account the major impact of the input voltage. Simulation results performed in Matlab-Simulink environment prove that the existing simple models with constant parameters can not predict the motor performance accurately in particular for variable speed applications. Swings of torque, hunting phenomenon, improvement of power factor by temporarily increasing the stator voltage and start up behavior of the hysteresis machine are some important issues which can accurately be analyzed by the proposed modeling approach.

**Keywords:** Dynamic Transient Model, Equivalent Circuit, Hysteresis Motor, Variable Parameters.

## 1 Introduction

Hysteresis motor is a type of synchronous machine which has found wide applications as small scale machines. Due to simple structure and some favorite features, this motor is being used in various fields such as navigation, chemical, weaving, and military industries [1], [2]. From construction point of view, the stator of the motor has the same conventional poly-phase winding, while the rotor is made of some rings of hysteresis material. Having constant torque during the run up, demanding a moderate start up current that is usually less than 180% of the full load current, and noiseless operation are some of the great advantages of the hysteresis motors. A hysteresis motor also can pull a wide range of loads with different inertia into

synchronism. Having such exclusive superiorities, they however suffer from some disadvantages such as high magnetizing current, low power factor, and low efficiency caused by parasitic losses. Another defect is the lack of a fixed synchronous speed, especially when the load varies [3], [4].

Unlike the permanent magnet machines, the rotor of hysteresis motor takes role as a temporary magnet [5]. Therefore, when the load changes suddenly, the rotor poles move on their surface, causing 3 to 5 Hz oscillations. This low frequency and slowly damped oscillation of speed is called hunting phenomenon [6]. The speed oscillation may introduce serious errors in many applications such as gyroscopes [7]. Another drawback is relatively long time needed to reach the synchronism.

When the hysteresis motors are built as prototypes, their dynamic transient analyses in the design stage are quite important [8]-[10]. This topic has been discussed in a few papers. In [11] the Finite Elements (FE) method is used for analyzing, but it is rather time consuming. Also in [4] another method is proposed with

---

Iranian Journal of Electrical & Electronic Engineering, 2008.

Paper first received on 20 May 2008 and revised on 29 Sep 2008.

\* The Authors are with the Faculty of Electrical and Robotic Engineering, Shahrood University of Technology, Shahrood, Iran.

E-mail: [darabi\\_ahmad@hotmail.com](mailto:darabi_ahmad@hotmail.com), [teymoor\\_ghanbari@yahoo.com](mailto:teymoor_ghanbari@yahoo.com), [rafiei@iee.org](mailto:rafiei@iee.org), [sanati.mohsen@gmail.com](mailto:sanati.mohsen@gmail.com).

\*\* The Author is with the Faculty of Electrical & Computer Engineering, University of Tehran, Tehran, Iran.

E-mail: [Lesani@ut.ac.ir](mailto:Lesani@ut.ac.ir).

much simplification that makes the model inaccurate for dynamic/transient analysis. In this paper, a linear model with time varying parameters is proposed to predict transient behavior of the hysteresis motors accurately. The paper is organized as follows:

The basic equations of the motor are presented in Section 2. In Section 3, the d-q equivalent circuits of the motor are given taking into account the exact effect of the hysteresis loops of the rotor material. In Section 4, the simulation results under various situations including the start up scenario are presented to prove the accuracy and suitability of the proposed model. Simulations of the study machine, which is a flat type hysteresis motor, are carried out in Matlab-Simulink environment. This section also explores how the hunting phenomenon along with some other performances of the machine can easily be predicted by the proposed model. Finally, Section 5 concludes the paper.

## 2 Electrical Model of the Hysteresis Motors

For modeling of the hysteresis motors, the following assumptions are made:

- 1- The stator winding is a sinusoidal distributed winding.
- 2- The magnetic flux in the air gap is axial whereas it is circumferential in the hysteresis material of the rotor.

- 3- Impact of the hysteresis loops, their changes (dynamic operating loop), and eddy currents all are taken into account.
- 4- Hysteresis loops of the rotor material are experimentally obtained by fitting the curves to the empirical data.

In Fig. 1, the schematic model of a typical 3-phase hysteresis motor with 3-phase stator windings and 120 degree displacement in the abc reference frame are shown [2].

In this model the hysteresis loop of the rotor can be replaced by 3-phase balanced windings with the same number of turns of the stator windings or two phase equivalent windings as shown in d-q frame of reference by Fig. 1. The eddy current effect on the performance of motor which depends on the slip is modeled by resistance  $R_e$ , and the hysteresis loss and power are represented by  $R_h$ . As shown in Fig. 1, the parameter  $\alpha$  is the angle between d axis and phase 'a' axis of the stator, which is called hysteresis delay angle. Also,  $V_{rd}$  and  $V_{rq}$  in Fig. 1 are the equivalent induced voltages for the hysteresis loop of the rotor. These voltages are constant at synchronous condition, when the flux densities become fixed all through the rotor.

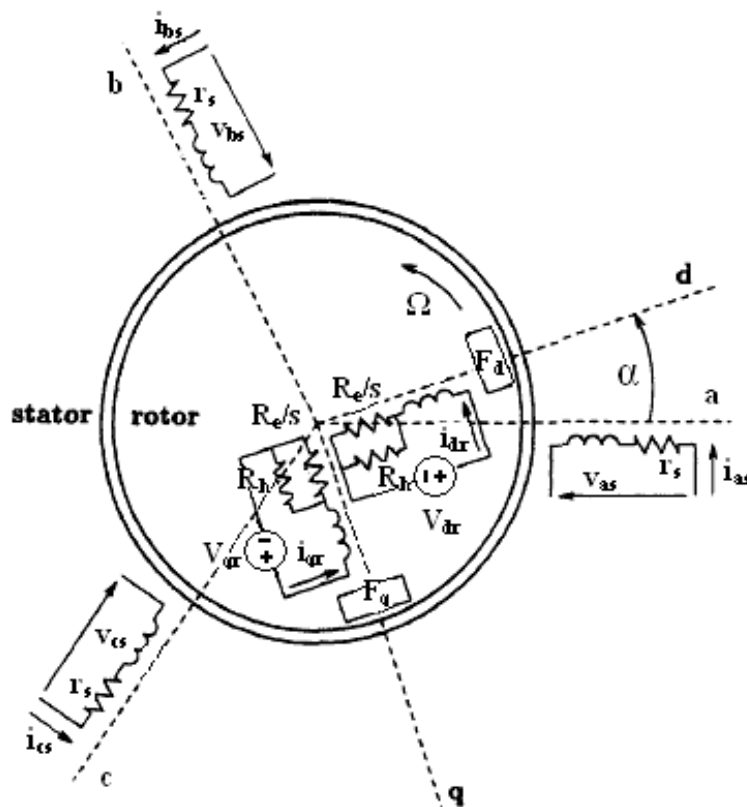


Fig. 1 Schematic model of hysteresis motors.

Rotor parameters in the above mentioned equivalent circuit model can be obtained from structural parameters of a disc type hysteresis motor which are given by equations (1)-(4) [10]:

$$R_h = \frac{4mf(K_w N_{ph})^2 t_r R_{oi} K_{sf} B_q \sin \alpha}{1000 R_{av} H_p} [\Omega] \quad (1)$$

$$X_r = \frac{R_h}{\tan \alpha} [\Omega] \quad (2)$$

$$R_e = \frac{48mp(K_w N_{ph})^2 R_{oi}}{2\pi R_i t_r} [\Omega] \quad (3)$$

$$r_r = \frac{R_h R_e}{s R_h + R_e} [\Omega] \quad (4)$$

If the stator equations are transferred to the rotor side, describing mathematical model of the hysteresis machine in the rotor reference frame can be derived as:

$$V = RI + \frac{1}{\omega_b} X_1 \dot{I} + \frac{\omega_r}{\omega_b} X_2 I \quad (5)$$

Equation (5) can be rewritten with more details as [4]:

$$\begin{bmatrix} V_{ds} \\ V_{qs} \\ V_{dr} \\ V_{qr} \end{bmatrix} = \begin{bmatrix} r_s & 0 & 0 & 0 \\ 0 & r_s & 0 & 0 \\ 0 & 0 & r_r & 0 \\ 0 & 0 & 0 & r_r \end{bmatrix} \begin{bmatrix} i_{ds} \\ i_{qs} \\ i_{dr} \\ i_{qr} \end{bmatrix} + \frac{1}{\omega_b} \begin{bmatrix} X_s & 0 & X_m & 0 \\ 0 & X_s & 0 & X_m \\ X_m & 0 & X_{rr} & 0 \\ 0 & X_m & 0 & X_{rr} \end{bmatrix} \begin{bmatrix} \dot{i}_{ds} \\ \dot{i}_{qs} \\ \dot{i}_{dr} \\ \dot{i}_{qr} \end{bmatrix} + \frac{\omega_r}{\omega_b} \begin{bmatrix} 0 & -X_{ss} & 0 & -X_m \\ X_{ss} & 0 & X_m & 0 \\ 0 & 0 & 0 & 0 \\ 0 & 0 & 0 & 0 \end{bmatrix} \begin{bmatrix} i_{ds} \\ i_{qs} \\ i_{dr} \\ i_{qr} \end{bmatrix} \quad (6)$$

All parameters of the motor used in this paper are given in table I. These equations can be summarized in

the equivalent circuit model [2] as shown in Fig. 2. In this figure,  $E_{od}$  and  $E_{oq}$  are defined by equations (7).

$$E_{od} = (1-s)[(X_s + X_m)i_{qs} + X_m i_{qr}] \quad (7a)$$

$$E_{oq} = (1-s)[(X_s + X_m)i_{ds} + X_m i_{dr}] \quad (7b)$$

Also, the electromagnetic torque of the hysteresis motor is given by (8).

$$T_{em} = \left(\frac{3}{2}\right)\left(\frac{p}{2}\right)(i_{qs} \lambda_{ds} - i_{ds} \lambda_{qs}) \quad (8)$$

where:

$$\begin{aligned} \lambda_{ds} &= \frac{1}{\omega_b} (X_{ss} i_{ds} + X_m i_{dr}) \\ \lambda_{qs} &= \frac{1}{\omega_b} (X_{ss} i_{qs} + X_m i_{qr}) \end{aligned} \quad (9)$$

And finally the motion equation for a p-pole hysteresis motor can be stated by (10).

$$2H \dot{\omega} = T_{em} - T_L \quad (10)$$

where:

$$\omega = \frac{\omega_r}{\omega_b}, \quad H = \frac{j\omega_b}{p} \quad (11)$$

### 3 Impact of Hysteresis Loops of Rotor

It is well known that when a hysteresis material is exposed to a sinusoidal field (H) with specified amplitude, the flux density (B) is non-sinusoidal and the corresponding B-H curve follows a hysteresis loop. By putting a small piece of the rotor material into experiment, it is possible to obtain the magnetic characteristics of the rotor substance. For this purpose, a toroidal core with rectangular cross section is designed from the rotor material with two coils on it supplied by a low frequency voltage with adjustable amplitude. While testing, voltages and currents of the coils are measured and processed by a PC computer.

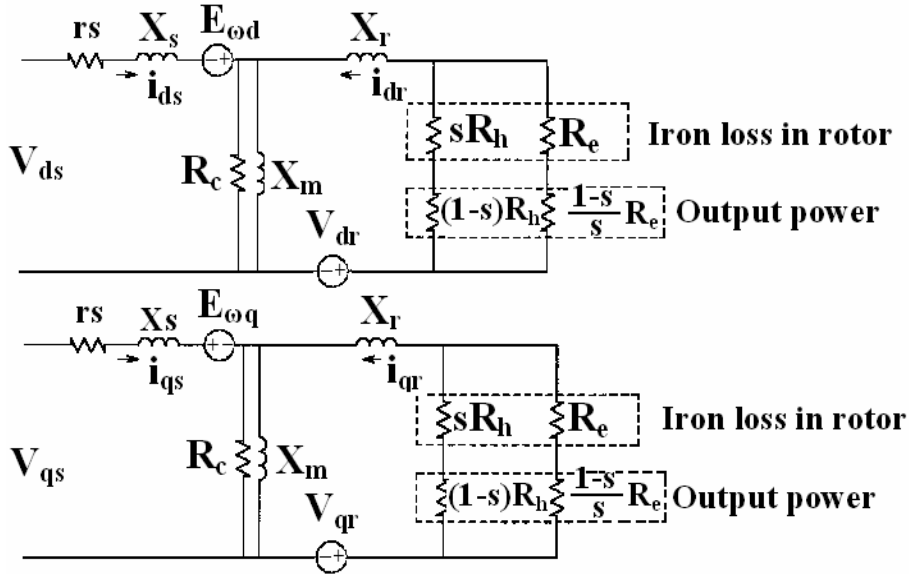


Fig. 2 Equivalent circuit of hysteresis motor in d-q references.

Then the hysteresis loops of the material are calculated. This test is done for alloy steel with compositions Fe-Cr-Ni-Mo-C and with particular heat treatment. Measured loops are depicted in Fig. 3. Maximum achievable output power of the motor in the steady state is proportional to the area of the corresponding operating loop as shown versus peak value of the field intensity in Fig. 4. If the fundamental harmonic of the magnetic field intensity is defined as  $H(t) = H_p \cos \omega t$ , then the fundamental harmonic of the flux density can be expressed as:

$$B(t) = a_1 \cos \omega t + b_1 \sin \omega t = B_q \cos(\omega t - \alpha) \quad (12)$$

where  $a_1$  versus  $H_p$  is shown in Fig. 5, the value of  $b_1$  for any given  $H_p$  can be calculated by  $b_1 = E_h / (\pi H_p)$ ,  $\alpha$  is the hysteresis delay angle and it is evaluated by  $\alpha = \text{Arctan}(b_1/a_1)$ , and  $B_q$  is the amplitude of fundamental harmonic of the flux density and is equals to  $B_q = \sqrt{a_1^2 + b_1^2}$ . In many reports  $\alpha$  is assumed constant for a given material [10], while this parameter varies greatly around its maximum value which is 42 degrees for the material used here.

During start-up, when a hysteresis motor is supplied by sinusoidal voltage, due to sweeping of the rotor substance by the stator flux, the hysteresis loss varies by the flux sweep frequency. The delay between the fundamental space harmonics of the rotor flux and the field intensity is equal to hysteresis delay angle. Therefore in this circumstances if the fundamental space

harmonic of the magnetic field intensity in the middle path of the rotor disk is defined as  $H = H_p \cos \theta$ , then the fundamental harmonic of the flux density can be written as:

$$B_1(\theta) = a_1 \cos \theta + b_1 \sin \theta = B_q \cos(\theta - \alpha) \quad (13)$$

where,  $\theta$  is the position angle of a given point of the rotor. When the input voltage is sinusoidal, the rotor substance somewhat follows just one of the B-H loops after a short transient time (approximately one cycle). Operating hysteresis loop is related to the amplitude of the input voltage. If there are some harmonics in the input voltage too, some minor loops appear on the operating loop with frequency of the harmonics.

In contrast to other conventional motors, the simulation results carried out in the steady state show that the hysteresis motor parameters are quite sensitive to the voltage variation. Variations of the parameters with input voltage variations of the study hysteresis motor are shown in Fig. 6. Such parameter variations should necessarily be taken into considerations when designing or dynamic and transient performance analysis of the hysteresis motors. As seen in Fig. 6,  $r_s$  is not related to the input voltage and  $X_s$ ,  $X_m$  can also be considered constant over a wide range around the operating point. But  $X_r$ ,  $R_h$  and  $R_c$  vary significantly with input voltage variations. So, an equivalent circuit model with constant parameters cannot yield to accurate responses.

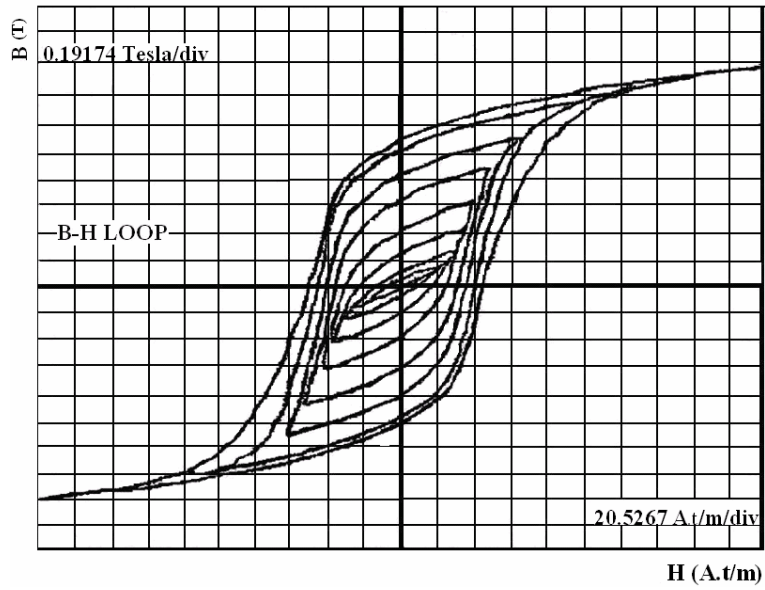


Fig. 3 Experimental hysteresis loops of the alloy steel of the rotor disc.

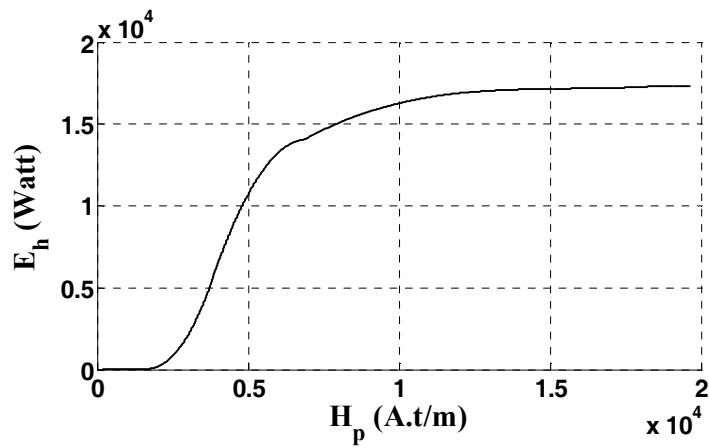


Fig. 4 Area of the hysteresis loops versus peak values of the field intensity.

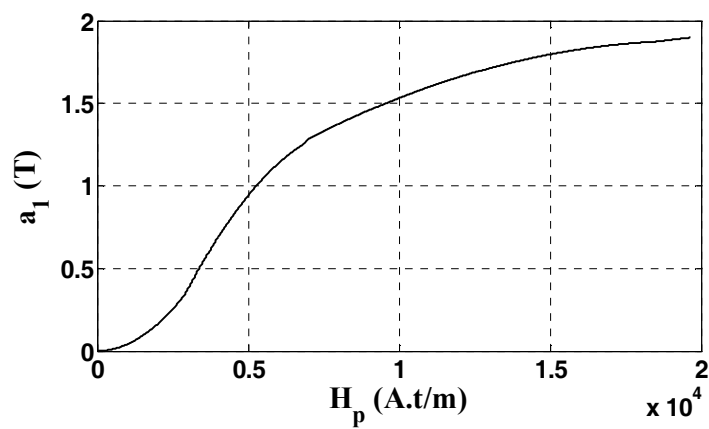


Fig. 5 Variation of  $a_1$  versus peak value of the field intensity.

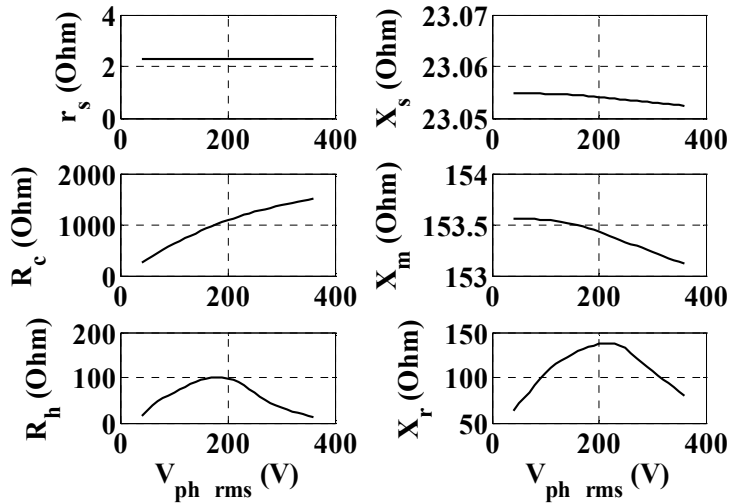


Fig. 6 Variations of the equivalent circuit parameters versus input phase voltage.

#### 4 Simulation Results of Transient Behavior of the Hysteresis Motor

It is well known that total torque of a hysteresis motor is produced via two different mechanisms, namely hysteresis torque and the eddy current torque. Hysteresis substance produces an angle between rotor mmf and the resultant air gap mmf. The difference between these fields causes a hysteresis torque, which is the dominant component of the total torque. Hysteresis power  $P_h$  in the hysteresis machines is almost constant. In the stationary state, total hysteresis power turns to heat, whereas it is the output power in the synchronous mode. The other torque is the induction torque, which is produced by eddy currents in the solid hysteresis material and its copper cover. This part is fairly considerable in accelerating the motor in the asynchronous regime.

The hysteresis motor under study is simulated according to equations (5)-(11) and the equivalent circuit presented by Fig. 2. The corresponding data are also given in table II.

In the model, expressed in d-q reference, the elements of the model are treated variable to reflect variations of the motor parameters discussed previously. Therefore the model is updated for any instant based on the information gathered from the instantaneous values of the voltage, slip, and the corresponding rotor operating loop. Suppose that initial flux intensity is  $H_p$  then  $B_q$  and  $\alpha$  are calculated as it is mentioned in the previews section.  $R_h$ ,  $X_r$  and  $R_c$  are determined by equations (1)-(3). Air gap flux ( $\Phi_g$ ), induced voltage ( $E_1$ ) and resultant air gap mmf ( $F_g$ ) are calculated respectively by:

$$\phi_g = 2t_r K_{sf} (R_o - R_i) B_q \times 10^{-6} \quad (14)$$

$$E_1 = \sqrt{2} \pi K_w N_{ph} f \phi_g \quad (15)$$

$$F_g = g \left( \frac{pt_r B_q}{2\mu_0 R_{av}} \right) \times 10^{-3} \quad (16)$$

Magnetic motive force and iron loss of the stator yoke and teeth and consequently the value of  $R_c$  can be determined by means of magnetic characteristics of stator core. By assuming the input phase voltage as reference, phasor of the input phase current can be obtained from:

$$I_{eq} = \sqrt{\left( \frac{E_1}{R_c} + I_h \sin \alpha \right)^2 + \left( \frac{E_1}{X_m} + I_h \sin \alpha \right)^2} \angle -\zeta \quad (17)$$

where:

$$\zeta = \text{Arc tan} \left( \frac{\frac{1}{X_m} + \frac{\cos \alpha}{Z_r}}{\frac{1}{R_c} + \frac{\sin \alpha}{Z_r}} \right), I_h = \frac{E_1}{Z_r}, Z_r = \sqrt{(r_r)^2 + X_r^2}$$

Input voltage is then calculated by:

$$V_{ph} = \sqrt{(E_1 \cos \zeta + Z_1 I_{eq} \cos \delta)^2 + (E_1 \sin \zeta + Z_1 I_{eq} \sin \delta)^2} \quad (18)$$

where:

$$Z_1 = \sqrt{r_s^2 + X_s^2} \quad \text{and} \quad \delta = \text{Arc tan} \left( \frac{X_s}{r_s} \right)$$

At this stage the calculated input voltage by equation (18) has to be equal to the real input voltage. Otherwise the value of  $H_p$  is modified by a proper step size and calculations are repeated until the difference between these two values falls into a given tolerance. Finally, phasor of  $E_p$  as equivalent voltage for hysteresis element is obtained by:

$$E_p = \sqrt{\frac{(X_m I_{eq} \sin \zeta + (X_r + X_m) I_h \sin \alpha)^2 + (X_m I_{eq} \cos \zeta + (X_r + X_m) I_h \cos \alpha)^2}{\sin^2 \alpha}} \angle -\gamma \quad (19)$$

where:

$$\gamma = \text{Arctan}\left(\frac{X_m I_{eq} \cos \zeta + (X_r + X_m) I_h \cos \alpha}{X_m I_{eq} \sin \zeta + (X_r + X_m) I_h \sin \alpha}\right)$$

Calculated  $E_p$  is a phasor for phase 'a', so it has to be written in time domain for each phase and transferred to synchronously rotating d-q reference frame to obtain  $V_{dr}$  and  $V_{qr}$ . Now all parameters of the machine are updated for this time.

## 5 Simulation Results

### 5.1 Motor without Load Under Nominal Supply

Speed and torque of the machine are depicted in Fig. 7 when the hysteresis machine is assumed to be no-load and it is driven by nominal voltage. The starting torque is around 0.5 Nm and the overall starting time is 2.5 s. Three phase input currents as well as the currents of to  $R_h$  and  $R_c$  in d-q frame, are shown in Fig. 8. The starting current swings up to twice the synchronous mode current, of course just for a short time-interval in

the beginning as it is apparent in the figure, the eddy current in both axes vanishes as the rotor speed approaches the synchronous speed.

If the loops switching was not taken into account, the simulation results of speed, torque and current would be as given by Fig. 9 [4]. According to Fig. 9 the ratio of start-up current to steady-state current is about 10 and the start-up time is 0.6 s. This current ratio seems too high while the start-up time is very short.

Through start-up, some parameters of the motor vary. The variations of the rotor equivalent resistors  $R_h$  and  $X_r$  due to changes in the hysteresis loops are illustrated in Fig. 10. Variations of these parameters can be verified by using equations (1) and (2). These parameters get fixed in steady state when there is no fluctuations in the flux density and the hysteresis loop either.

### 5.2 Motor without Load and with 60% of Nominal Voltage

Some important characteristics of the no load motor but supplied by 60% of the nominal voltage are illustrated in Fig. 11. As it is seen from Fig. 11, the motor can start and pull into synchronism by the input voltage less than the nominal voltage with no problem, which is impossible for many other types of synchronous motors. This reduction in the voltage decreases the starting torque to about 0.2 Nm, and significantly increases the starting time from 2.5 seconds to 7 seconds. The speed fluctuations in the beginning of the start-up process are apparently more significant where the lower voltage supply is applied. When the machine is supplied with nominal voltage, the rotor currents in the stationary reference are shown in Fig. 8.

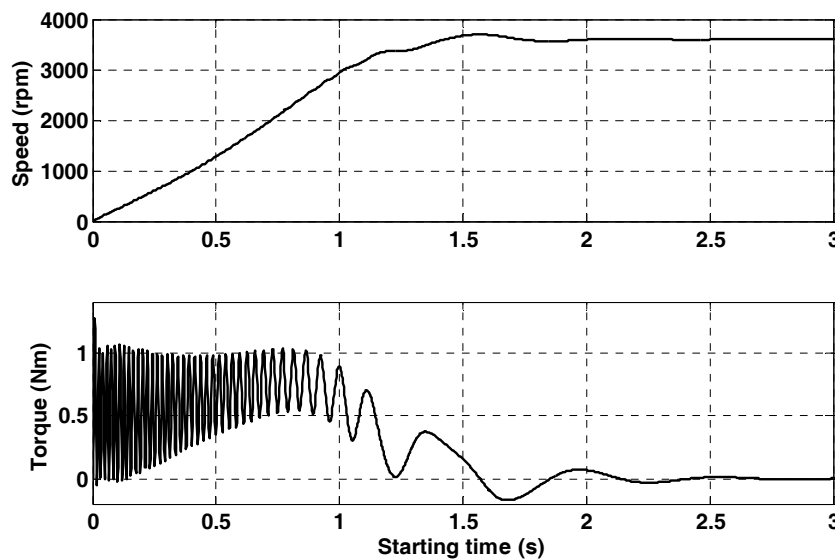


Fig. 7 speed and torque, in no load condition with nominal supply voltage.

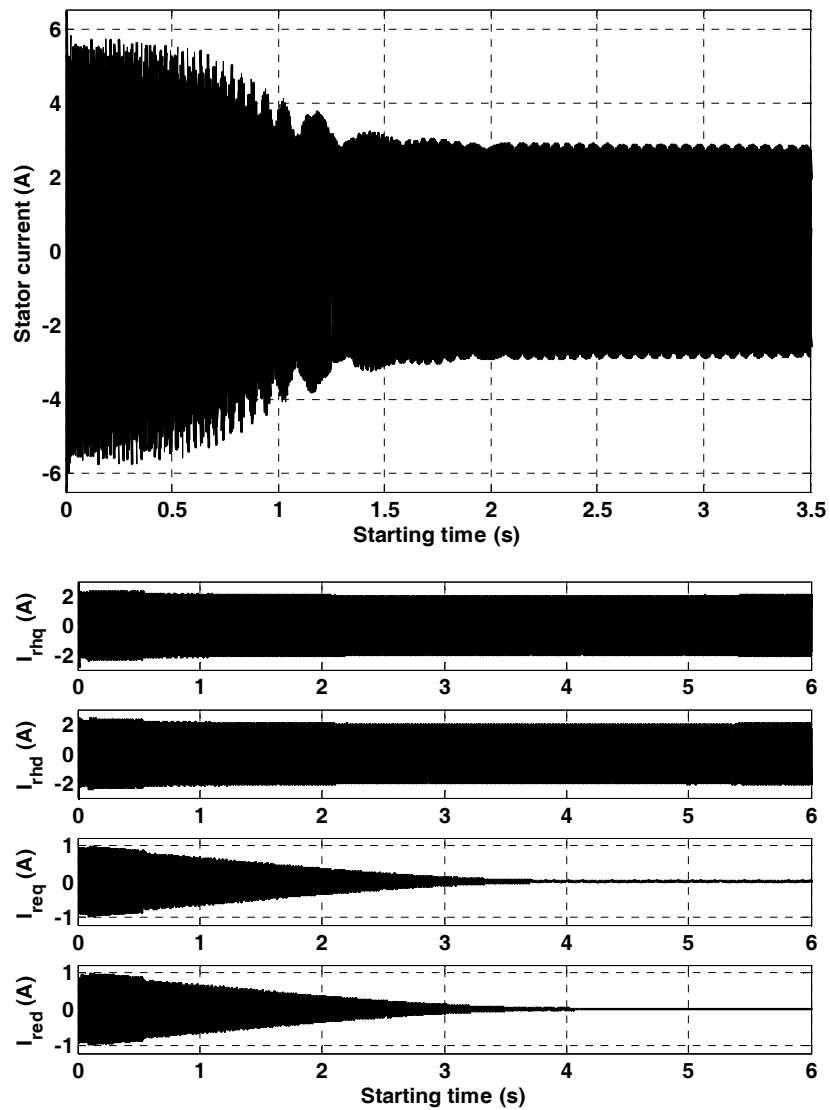


Fig. 8 Three phase Input currents and rotor currents in no load condition with nominal supply voltage.

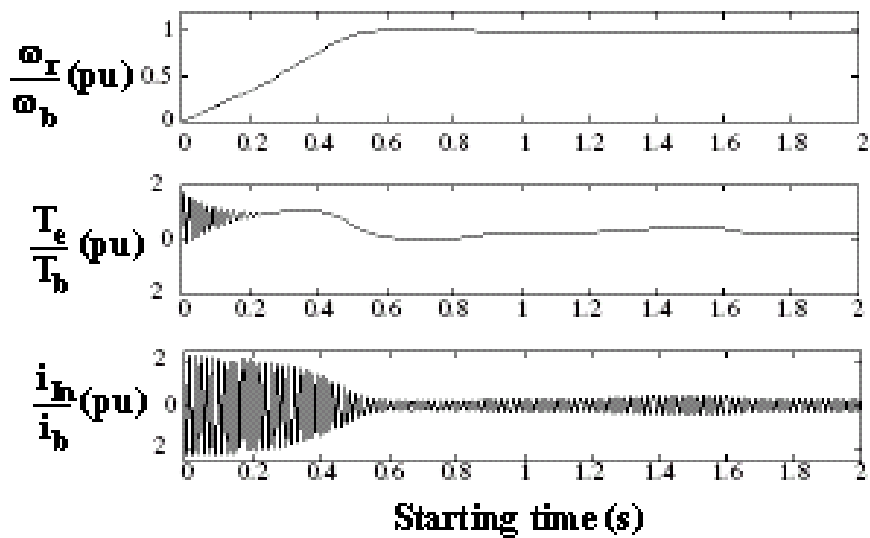


Fig. 9 Speed, torque and input currents of no load hysteresis motor supplied with nominal voltage [4].

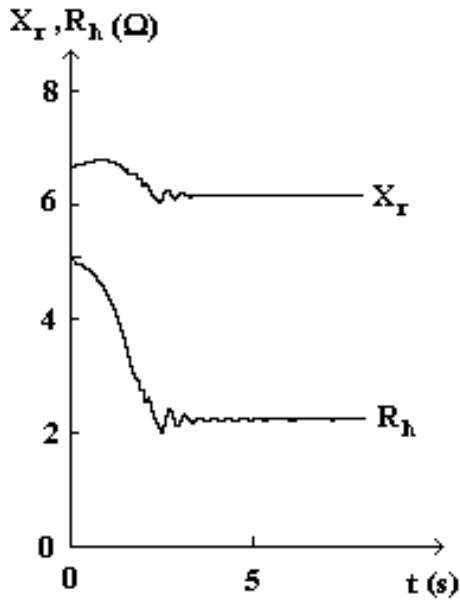


Fig. 10 Variations of  $R_r$ ,  $X_r$  in no load condition with nominal supply voltage.

They are also depicted for 60% of the nominal voltage in rotor reference frame in Fig. 11.

It can be seen in Fig. 12 that the motor acts as a permanent magnet machine in the synchronous mode with a constant rotor current. Being random, the current levels of d and q axis depends on the position of the rotor in the synchronism state which is a random quantity as well.

Torque characteristic of the motor versus speed for nominal voltage and for 60% of the nominal voltage are also shown in Fig. 13. This figure explores that the torque fluctuations frequency is higher and its damping speed is lower for the lower voltage case. So it can be inferred that for reducing the start-up time applying a short-term voltage higher than the nominal voltage may be useful. Also, small increase of the voltage or over excitation is also possible at synchronous speed, which is expected to improve the overall performance of the motor. As already mentioned, low power factor characteristics of the hysteresis machines is a major concern.

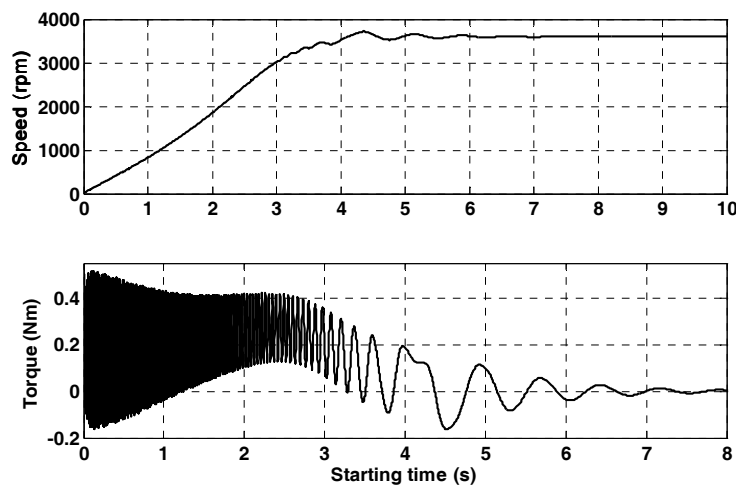


Fig. 11 Speed and torque of no load hysteresis motor supplied with 60% of the nominal voltage.

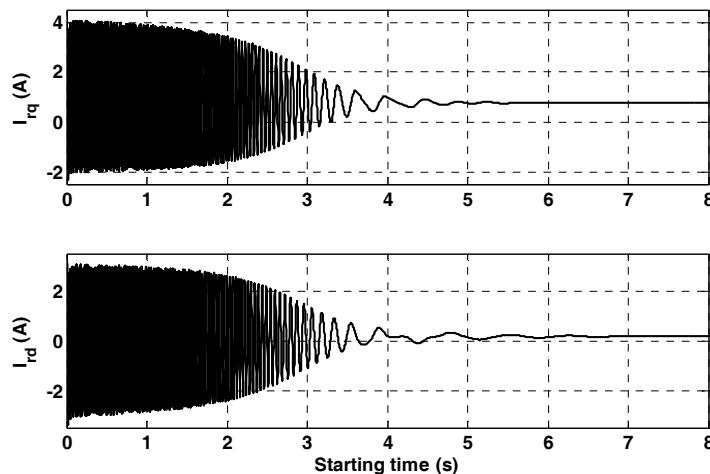
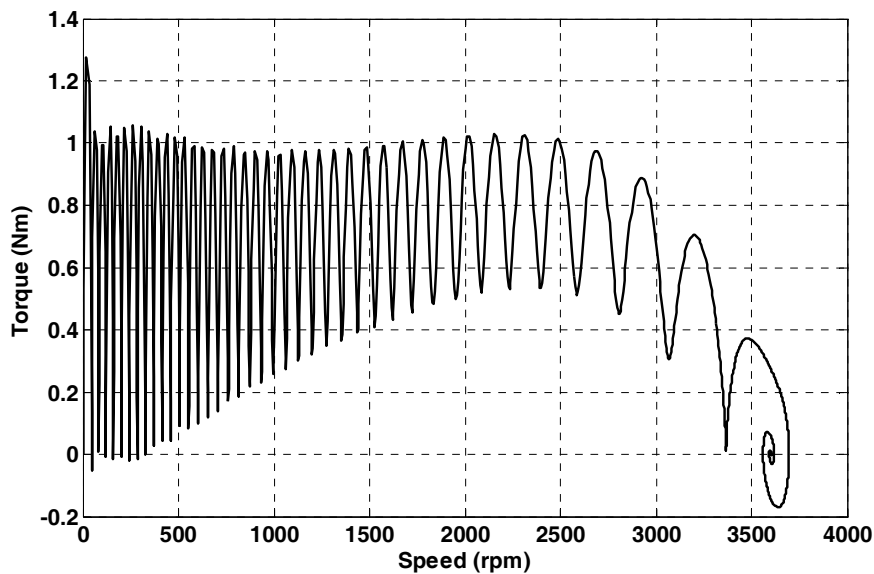
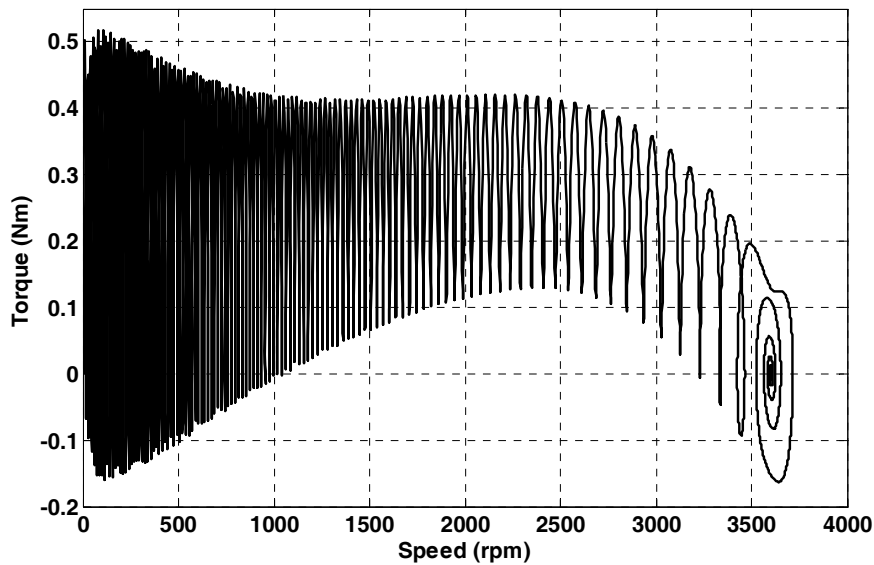


Fig. 12 Rotor currents in d-q reference for no load hysteresis motor supplied with 60% of the nominal voltage.



(a)



(b)

**Fig. 13** Torque versus speed under (a) nominal input voltage (b) 60% of the nominal input voltage.

However, as addressed in [12], the power factor and efficiency can sufficiently be improved through reducing the supply voltage of the motor at cost of some torque reduction. For instance, as illustrated in Fig. 14, when the supply voltage decreases to 60% of the nominal value, it would increase the power factor from 0.31 to 0.36.

### 5.3 Torque and Speed Variation During Step Load Application

Graphs of the torque and speed are illustrated in Fig. 15. The motor is initially started up at nominal voltage with a 0.1 Nm load and then a step load of 0.2 Nm is applied at 4 s.

As seen from the figure, any sudden change in the load at synchronism produces some expected low damped fluctuations in the speed and torque. This phenomenon which is called hunting is one of the hysteresis motor disadvantages. These fluctuations usually appear with a frequency of 3 to 5 Hz around the operating point. The input voltage changing is usually causes hunting phenomenon too. The hunting phenomenon can more clearly be traced in the enlarged Fig. 16. This phenomenon is expected to be more serious for higher power motors. Furthermore, where the load increase is not significant and the motor can accelerate it successfully, then the speed remains nearly constant.

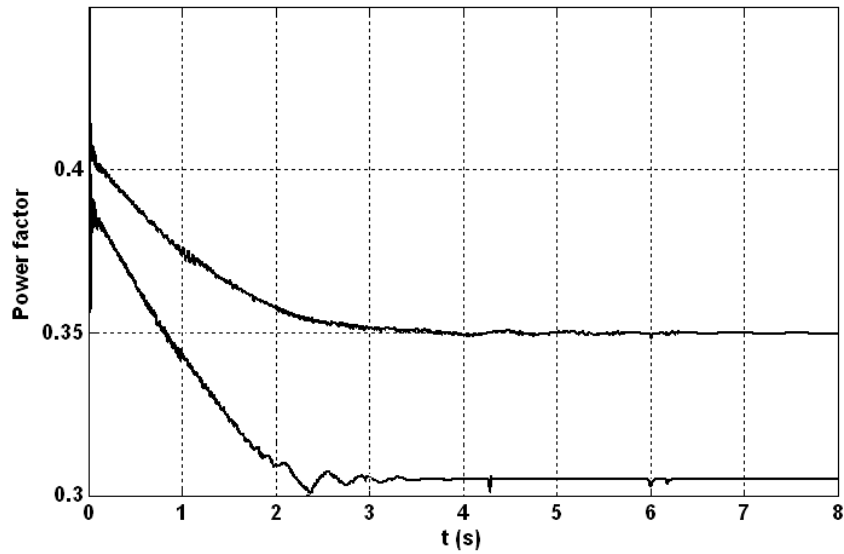


Fig. 14 Power factor A) nominal voltage B) 60% of nominal voltage.

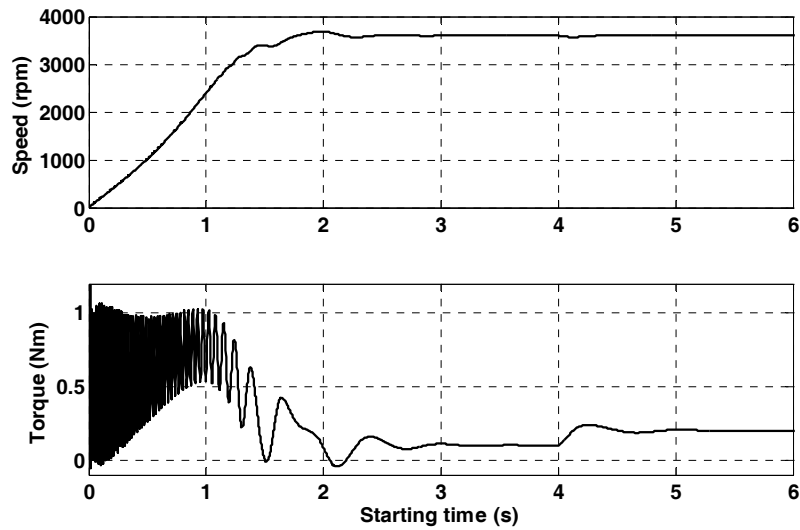


Fig. 15 Speed and torque variations caused by step load application from 0.1 Nm to 0.2 Nm in synchronism.

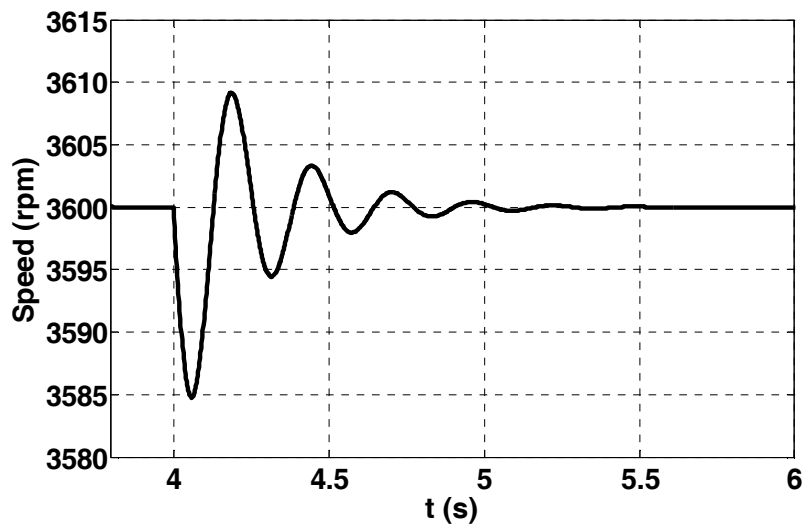


Fig. 16 Magnified speed oscillations (hunting phenomena) caused by step load.



**Fig. 17** Photos of two hysteresis motors.

But if the produced torque fails to compensate the load change, the motor will run as an asynchronous motor, operating at a speed less than the synchronous speed. Another interesting feature of these motors is the fact that the load increase at synchronism does not cause any major change in the input current amplitude. Fig. 12 explains the matter very well. In other words, having almost constant speed and current amplitude in addition to low start-up current are some interesting advantages of hysteresis motors verified in this paper based on the new modeling approach.

#### 5.4 Some Experimental Results

Several types of the hysteresis motor are manufactured in our workshop; the photos of two motors are shown in Fig. 17.

Unfortunately, due to no access to a suitable data acquisition set, experimental results of transient cannot be derived accurately and only some steady state experimental results are reported. When the motor works in no load condition with about 50 watts friction loss, the steady state current and start up time at nominal input voltage have experimentally measured as 3.1 A and 2.5 s respectively. Furthermore power factor in this condition is 0.3 which are proven the simulation results.

The model presented for a similar size machine in [4] predicts the start up and steady state currents as 10 A and 4 A, respectively under the same condition considered in this paper. The starting time is also predicted to be around 0.5 s which reveals the modeling error. The results as well as the discussion mentioned earlier prove the overall superiority of the proposed model in this paper.

## 6 Conclusion

A dynamic transient model in Matlab/Simulink environment is proposed based on direct utilizing the equations of hysteresis motor taking into consideration the dynamic hysteresis loops and output characteristics of the model in different conditions. Comparison of the

results obtained from three different case studies in this paper with those obtained experimentally [1], [3], validates the accuracy of the proposed modeling approach, while this method takes less simulation time in comparison to well-known FE method. Having constant speed and torque with low start-up current are some outstanding properties of hysteresis motors which were clearly investigated in the paper. On the other side, high starting time, high frequency and less damped fluctuations of speed at start up with input voltage less than the nominal, and also hunting phenomenon are some of the hysteresis motors disadvantages investigated by the proposed modeling approach accurately. Power factor correction by voltage supply reduction is also addressed in this paper. Furthermore, the modeling approach proposed by this paper predicts almost all important characteristics of the hysteresis motors which can be used for optimal design and control of the machine with fast execution time.

## Appendix

In table I all of the used parameters are introduced and in table II the hysteresis motor parameters are presented.

**Table I** Nomenclature.

$V_{ds}, V_{qs}$	Stator voltage in d-q axis
$V_{dr}, V_{qr}$	Rotor voltage in d-q axis
$r_s, r_r$	Stator and rotor resistance
$X_s, X_r$	Leakage reactances of stator and rotor
$X_{ss}, X_{rr}$	Total reactances of stator and rotor
$X_m$	Magnetizing reactance
$I_{ds}, i_{qs}$	Stator currents in d-q axis
$I_{dr}, i_{qr}$	Rotor currents in d-q axis
$\omega_r$	Angular speed of rotor
$\omega_b$	Basic angular speed
$T_{em}$	Electromagnetic torque

$\lambda_d, \lambda_q$	Linkage fluxes in d-q axis
$T_L$	Load torque
H	Rotor inertia constant
s	Slip
$K_{sf}$	Stacking factor of stator laminations
$t_r$	Thickness of rotor disk [mm]
$K_w$	Winding factor
$N_{ph}$	No. of turns per phase
m	Number of phases
$R_o$	Inner radius of rotor and stator [mm]
$R_i$	Outer radius of rotor and stator [mm]
$R_{oi}$	$R_o - R_i$
g	Axial air gap between stator and rotor [mm]
$R_{av}$	$(R_i + R_o)/2$
$\rho$	Resistivity of hysteresis material

**Table II** Motor parameters.

$P_{out} = 50$ watt	F = 60 Hz
$r_s = 2$ $\Omega$	P = 2
$L_s = 0.0086$ H	H = 0.4
$L_m = 0.0504$ H	$V_{ph} = 80$ volt

## References

- [1] Kazaumi K. and Azizur Rahman M., "Transient performance analysis synchronous motor," *IEEE Trans. On INDUSTRY App.*, Vol. 4, No. 1, pp. 135-142 Jan./Feb. 2004.
- [2] Azizur Rahman M. and Ruifeng Q., "Starting and synchronization of permanent magnet hysteresis motors," *IEEE Trans. On INDUSTRY App.*, Vol. 32, No. 5, pp. 1183-1189, Sep./Oct. 1996.
- [3] Azizur Rahman M. and Osheibba A., "Dynamic performance prediction of poly phase hysteresis motors," *IEEE Trans. On INDUSTRY App.*, Vol. 26, No. 6, pp. 1026-1032, Nov./Dec., 1990.
- [4] AWed Badeb O. M., "Investigation of the dynamic performance of hysteresis motors using MATLAB/SIMULINK," *Journal of Electrical Engineering*, Vol. 56, No. 3-4, pp. 106-109, 2005.
- [5] *Properties and selection of metals*, 8<sup>th</sup> Edition, ASM International, Lyman T., Vol. 1, pp. 1217-8, 1961.
- [6] Clurman S., "On hunting in hysteresis motors and new damping techniques," *IEEE Trans. on Magnetism*, Vol. 7, No. 3, pp. 512-517, Sep. 1971.

- [7] Rajagopal K. R., "Design of a compact hysteresis motor used in a gyroscope," *IEEE Trans. on Magnetism*, Vol. 39, No. 5, pp. 3013-3015, 2003.
- [8] Walker P., "A method for designing and analyzing hysteresis motor," *IEEE Conf. Paper, Winter Meeting*, No. 6830P36-PWR, 1968.
- [9] Selemo G. R., Jackson R. D. and Rahman M. A., "Performance predictions for large hysteresis motor," *IEEE Tran. on Power Apparatus And Systems*, Vol. PAS-96, No. 6, pp. 1915-1919, Nov./Dec. 1977.
- [10] Ishikawa T. and Kataoka T., "Basic analysis of disk type hysteresis motor," *Electrical Engineering in Japan*, Vol. 101, No. 6, pp. 659-666, 1982.
- [11] Kim H. K., Jung H. K. and Hong S. K., "Finite element analysis of hysteresis motor using the vector Magnetization-Dependent method," *IEEE Trans. on Magnetism*, Vol. 34, No. 5, pp. 3495-3498, Sept. 1998.
- [12] Copland M. A. and selemo G. R., "Analysis of hysteresis motor," *AIEE Fall General Meeting*, part one, pp. 34-41, Apr. 1964.



**Ahmad Darabi** received the B.Sc. degree in Electrical Engineering from Tehran University, Tehran, Iran in 1989 and the M.Sc. degree in the same field from Ferdowsi University, Mashhad, Iran, in 1992. He obtained the Ph.D. degree with the Electrical Machine Group, Queen's University, Belfast, UK, in 2002. He is now an Assistant

Professor and has been with Faculty of Electrical and Robotic Engineering, Shahrood University of Technology, Iran from 1993. His research activities were mostly on design, modeling and manufacturing of miniature electrical machines and generating sets.



**Teymoor Ghanbari** was born in Koohdasht, Iran in 1971. He received the B.Sc. degree in the Electrical Engineering in 1998 from Shahid Rajaei University, Tehran, Iran. He got his M.Sc. degree in the Electrical Engineering in 2007 from Shahrood University of Technology, Shahrood, Iran. He works on electrical machines, power

electronics and drives.



**Mohammadreza Rafiei** was born in 1969 in Tehran, Iran. He received B.Sc. degree with honor from the Sistan and Baluchistan University, Zahedan, Iran, in 1991, M.Sc., and Ph.D. degrees from the Ferdowsi University of Mashhad, Mashhad, Iran, in 1995 and 2000 respectively all in Electrical Engineering. He is currently with the Faculty of

Electrical Engineering of Politecnico Di Torino, Turin, Italy as a Senior Researcher. Dr. Rafiei is Senior Member of IEEE and member of IEEE Control Systems, Power Electronics, Signal Processing, and Power Engineering societies. His field of interests includes Control Systems, Power Electronics, Power System Dynamics, and Power Quality.



**Mohsen Sanati-Moghadam** was born in Yazd, Iran in 1981. He received the B.Sc. degree in Electrical Engineering in 2005 from Yazd University, Yazd, Iran. He got a M.Sc. degree in the Electrical Engineering in 2008 from Shahrood University of technology, Shahrood, Iran. He works on the rotating electrical machine design and

derives systems.



**Hamid Lesani** received the M.Sc. degree in Electrical Power Engineering from the University of Tehran, Tehran, Iran, in 1975, and the Ph.D. degree in Electrical Engineering from the University of Dundee, U.K., in 1987. Early in his career, he served as a Faculty Member with Mazandaran University. After obtaining the

Ph.D. degree, he joined the Department of Electrical and Computer Engineering, Faculty of Engineering, University of Tehran, where he is a Professor. His teaching and research interests are design and modeling of electrical machines and power systems. Professor Lesani is a member of IEEE (PES) and IEEE Iran Section.